OPTIMAL CONTROL APPLICATIONS AND METHODS
Optim. Control Appl. Meth. 2011; **32**:350–368
Published online 5 July 2010 in Wiley Online Library (wileyonlinelibrary.com). DOI: 10.1002/oca.947

Hamiltonian two-degrees-of-freedom control of chemical reactors

Vicente Costanza*, † and Pablo S. Rivadeneira

Instituto de Desarrollo Tecnológico para la Industria Química (UNL-CONICET), Güemes 3450, 3000 Santa Fe, Argentina

SUMMARY

A novel unified approach to two-degrees-of-freedom control is devised and applied to a classical chemical reactor model. The scheme is constructed from the optimal control point of view and along the lines of the Hamiltonian formalism for nonlinear processes. The proposed scheme optimizes both the feedforward and the feedback components of the control variable with respect to the same cost objective. The original Hamiltonian function governs the feedforward dynamics, and its derivatives are part of the gain for the feedback component. The optimal state trajectory is generated online, and is tracked by a combination of deterministic and stochastic optimal tools. The relevant numerical data to manipulate all stages come from a unique off-line calculation, which provides design information for a whole family of related control problems. This is possible because a new set of PDEs (the variational equations) allow to recover the initial value of the costate variable, and the Hamilton equations can then be solved as an initial-value problem. Perturbations from the optimal trajectory are abated through an optimal state estimator and a deterministic regulator with a generalized Riccati gain. Both gains are updated online, starting with initial values extracted from the solution to the variational equations. The control strategy is particularly useful in driving nonlinear processes from an equilibrium point to an arbitrary target in a finite-horizon optimization context. Copyright © 2010 John Wiley & Sons, Ltd.

Received 3 November 2009; Revised 9 March 2010; Accepted 10 May 2010

KEY WORDS: optimal control; chemical reactors; nonlinear dynamics; optimization; two-degrees-of-freedom control; Hamiltonian systems

1. INTRODUCTION

Nonlinearities in chemical reactor dynamics pose challenging control problems, especially when multiple criteria of optimization are present. The phase-plots of steady-states for nonlinear dynamics adopt different patterns, sometimes leading to bifurcations, limit cycles, or strange attractors in high dimensions [1, 2]. These patterns may change, even structurally, when parameters of the dynamics vary (equilibrium control values may be regarded as parameters, especially when each manipulated variable is proportional to some physical variable like temperature or flow rate [3]). Consequently, changing operation from one steady-state to another as in chemical reactors, or attempting to reach a desired final state in some optimal sense as in batch operations, or regulation when strong deviations are present, may imply working near periodic orbits or bifurcation points, where model information and accurate control are essential. Moreover, for some chemical reactors, the graph of equilibrium control values contains closed curves in phase space, situation described as 'system with input multiplicities' in the literature. Therefore, changes in set-point not always

*Correspondence to: Vicente Costanza, Instituto de Desarrollo Tecnológico para la Industria Química (UNL-CONICET), Güemes 3450, 3000 Santa Fe, Argentina.
†E-mail: tsinoli@santafe-conicet.gov.ar

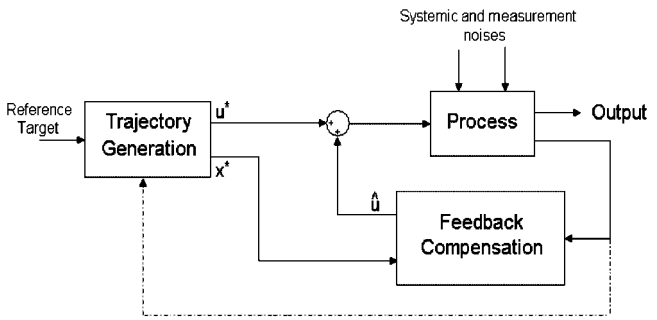

Figure 1. Two-degrees-of-freedom control design.

involve changes in the final equilibrium value of the manipulated variable (a parameter whose value may have been optimized *a priori*). These types of behavior present severe operation problems and demonstrate the need for feedback control, particularly when the process is open-loop unstable or when it exhibits nonlinear oscillations [4]. Other common process characteristics that cause control difficulty for nonlinear systems are multivariable interaction between manipulated and controlled variables, unmeasured states and frequent disturbances in the input–output signals [5].

Chemical reactors are usual classical examples in the nonlinear control literature ([2, 6–8], and their references). Several nonlinear advanced techniques have been developed (and these can be consulted in an extensive survey done by Bequette [5]), where the resulting controls were either linear or nonlinear. It is clear that nonlinear control in CSTR becomes more important if set-point changes are made, since significant departures from equilibrium are most probable to occur. Other (not necessarily equilibrium) points may be desirable to achieve, as it happens in batch processes. In such situations, both the nominal trajectory and its tracking must be optimized until a stop condition is reached in a finite time.

Apart from heuristic methods, there is a range of model-based approaches such as Model Predictive Control (MPC), which is becoming the most widely quoted in the recent literature. This method is essentially numerical, usually implemented online, but it requires significant computer capacity and speed. Most successful industrial applications of MPC reported so far are in refining and petrochemical plants, where processes are run near optimal steady-states and model linearizations are reliable approximations. Only a few of the available commercial software packages are cautiously suggested for truly nonlinear or batch processes [9], although recent applications of nonlinear MPC have been reported (see for instance [10–12]).

In this paper, the scheme shown in Figure 1 is adapted to the optimal control framework. This scheme integrates feedforward and feedback characteristics in a technique called 'two-degrees-of-freedom (2DOF) design', which is preferred when both the construction of a reference trajectory, and its tracking or disturbance attenuation are required (see [13, 14]). The resulting structure succeeds in obtaining: (i) optimal reference trajectory generation by means of a feedforward control and (ii) robustness toward disturbances by means of a feedback control. The 2DOF structure has been adapted to various frameworks and applied to CSTR reactors. In [15], steady-state and local asymptotic stability of a closed-loop system are obtained. However, the methodology is analyzed on the basis of new variables resulting from the global linearization of the nonlinear system, and as a consequence part of the physical interpretation is missed.

The main features of the approach presented here are: (i) the nominal trajectory is optimal and generated online, and (ii) the compensation stage is designed under the same optimization criteria used from the beginning. Instead of an arbitrary reference curve, the state trajectory is a solution of the Hamiltonian canonical equations (HCEs), which handle all nonlinearities of the process. This integration is possible due to recently discovered partial differential equations (PDEs) relating boundary conditions of the HCE to design parameters T, S (T: time horizon, S: final penalty matrix, see [16, 17] and the appendix for details). An optimal filter is used to generate the feedback compensation based on the error $\hat{x} = x - x_{\mathrm{d}}$, where x_{d} is the desired state (in this paper, x_{d} will

DOI: 10.1002/oca

be the optimal state trajectory x^*). In particular, the optimal estimate of the deviations $\hat{x}$ (in the least-squares sense) is the solution to the Kalman–Bucy differential equation (see [19] for details).

An application of the optimal 2DOF control scheme is presented for the nonlinear reactor model [4]. The equations correspond to an irreversible chemical reaction taking place in a perfectly mixed container. There are clearly two variables in the example that may be controlled, and just one variable (a flow rate) available for manipulation. No I/O pairing is possible since both states must be optimized. States are predicted through the solution to the HCEs, which are run in parallel.

The paper has the following structure: in Section 2, the main problem is introduced and a brief description of the 2-dimensional chemical process model and its dynamics are presented. Section 3 develops the PDEs equations to find the missing boundary conditions in the Hamiltonian problem. In Section 4, white input/output noises are included. The whole control strategy to eliminate such noises is posed. Finally, the complete approach is reviewed and condensed in the conclusions. An appendix is added to substantiate the new first-order PDEs used to calculate: (i) the missing initial costate needed to generate the optimal trajectory, and (ii) the initial condition for the Riccati matrix included in the compensator gain and the filter coefficients.

2. A CONTINUOUS STIRRED-TANK REACTOR (CSTR) WITH AN EXOTHERMIC REACTION

The case-study is an exothermic irreversible first-order reaction ($A \to B$), modeled through a set of two nonlinear ordinary differential equations obtained from dynamic material and energy balances (with the assumptions of constant volume, perfect mixing, negligible cooling jacket dynamics, and constant physical parameters) [4]. The dimensionless equations in composition (x_1) and temperature (x_2) are

$$\begin{aligned} \dot{x}_1 &= -\theta x_1 \exp\left(\frac{x_2}{1+x_2/\gamma}\right) + (q_0+u)(x_{1f}-x_1), \\ \dot{x}_2 &= \theta\beta x_1 \exp\left(\frac{x_2}{1+x_2/\gamma}\right) - \delta x_2 + (q_0+u)(x_{2f}-x_2). \end{aligned} \tag{1}$$

Typical values for the parameters are: $\theta=0.135$, $\gamma=20.0$, $x_{1f}=1.0$, $\beta=11.0$, $x_{2f}=0.0$, and $\delta=1.5$. The independent variable is $\tau=t/t_c$, where t is the physical time and t_c a characteristic time of the reactor. For the parameter values used here, t_c is in the order of 1 min (see [4, 19]). Each numerical simulation has consumed computer time in the order of 1 s, which indicates that online calculations can readily be implemented. It has been assumed that the external cooling dynamics is much slower than the reaction rate, and that the dimensionless feed flow rate q is the only variable to be manipulated. When the cooling jacket dynamics became relevant, then the reactor model becomes a multiple-input and multiple-output (MIMO) system, with the cooling rate as the second control variable. Such a case will not be treated here. Usually it is chosen to conduct operation around a fixed value q_0 of the flow-rate, and then an appropriate definition for the control variable would be $u=q-q_0$.

In Figure 2, the phase plane plot corresponding to system (1) for $q_0=3$ shows the qualitative behavior associated with multiple equilibria for a fixed value of the parameter q_0. Since q_0 is the dimensionless flow rate, an operational problem arises when trying to change the (state) set-point without changing the final value of q (possibly dictated by the steady-state functioning of the rest of the plant). This is because the state trajectory must navigate through potentially adverse conditions as the structure of the flow changes.

There are three equilibria, shown in Figure 2:

$$x_a = \begin{pmatrix} 0.9316 \\ 0.5014 \end{pmatrix}, \quad x_b = \begin{pmatrix} 0.4979 \\ 3.68153 \end{pmatrix}, \quad x_c = \begin{pmatrix} 0.1776 \\ 6.0306 \end{pmatrix},$$

where x_a and x_c are stable steady-state points and x_b is unstable.

DOI: 10.1002/oca

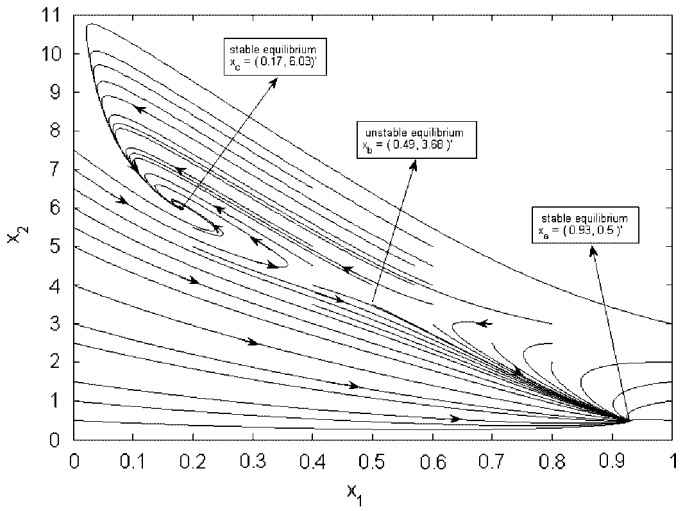

Figure 2. Phase plane for $q_0 = 3$.

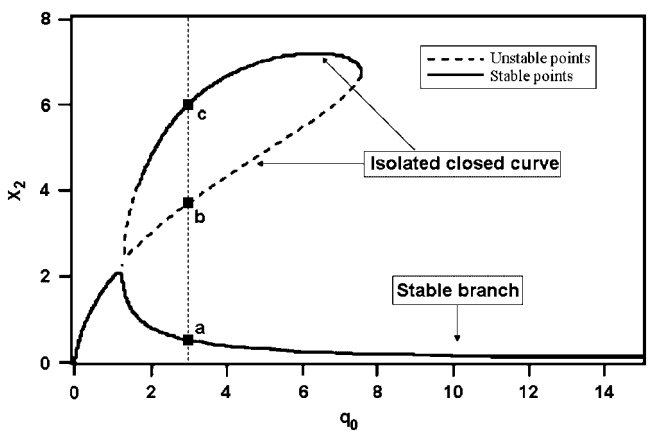

Figure 3. Input–output relationship for the exothermic CSTR.

This reactor exhibits both input and output multiplicities as shown in Figure 3. The input multiplicity can be seen on both the lower steady-state curve and in the isola (a closed, isolated loop of solutions from the steady-state input–output curve at a well-defined bifurcation point). The presence of 'isola' behavior in the classic two-state CSTR model is well-documented ([20] and the references therein). In Figure 3, the dashed line shows how the steady-state process gain has a different sign on the lower operating curve and at the top and bottom of the isola. The process is open-loop stable along the lower operating curve (or along the stable branch).

The presence of input multiplicities (multiple inputs for a given output) and isolas in a system severely degrades the performance of feedback controllers. For example, at the 'peak' of the steady-state curve the input–output gain is zero; hence, the system is inherently uncontrollable [4]. Output multiplicities (like in this reactor) require a sophisticated analysis when designing the control strategy, because the flow of the system is qualitatively more complex than those for classical linear systems. An example of this consideration is the following: if the initial condition is near x_b (in Figure 2), then there is no certainty on whether the equilibrium control $\bar{u} = 0$ would drive the system toward x_a or x_c. Consequently, an alternative control strategy needs to be devised by taking into account the desired final state.

DOI: 10.1002/oca

3. EQUATIONS FOR REGULAR OPTIMAL CONTROL PROBLEMS IN THE NONLINEAR CONTEXT

3.1. The Hamiltonian formalism for nonlinear systems and general costs

In this section, only initialized autonomous control systems of the nonlinear form

$$\dot{x} = f(x, u), \quad x(0) = x_0 \tag{2}$$

will be considered. The state x moves into some region $\mathscr{O}$ of $\mathbb{R}^n$, and the admissible control strategies are the real, piecewise continuous functions of the time-domain $\mathscr{T}$ into some open subset $\mathscr{U}$ of $\mathbb{R}^m$. The right-hand-side $f : \mathscr{O} \times \mathscr{U} \to \mathbb{R}^n$ is assumed to be smooth enough so as to guarantee existence and uniqueness of solutions to the dynamics equation (2) in the range of interest. The (finite-horizon) quadratic final penalty optimization context will imply that a cost functional like

$$\mathscr{J}(T, 0, x_0, u(\cdot)) = \int_0^{\mathrm{T}} L(x(\tau), u(\tau))\,\mathrm{d}\tau + x'(T)Sx(T) \tag{3}$$

has to be minimized on the set of admissible control trajectories, where $\mathscr{T} = [0, T]$, $T < \infty$, L is a nonnegative smooth arbitrary function called the Lagrangian of the problem, and S is called the final penalty coefficient. The value function $\mathscr{V}$ can always be defined for such a problem, namely

$$\mathscr{V}(t, x) \triangleq \inf_{u(\cdot)} \mathscr{J}(T, t, x, u(\cdot)), \quad t \in [0, T], \tag{4}$$

and if the problem has a unique solution, then it is called the optimal control strategy u^*,

$$u^*(\cdot) \triangleq \arg\inf_{u(\cdot)} \mathscr{J}(T, t, x, u(\cdot)), \tag{5}$$

which in turn will generate the optimal state trajectory

$$x^*(\cdot) \triangleq \text{solution to (2) with } u(\cdot) = u^*(\cdot). \tag{6}$$

The Hamiltonian $\mathscr{H}$ of such a problem is defined as

$$\mathscr{H}(x, \lambda, u) \triangleq L(x, u) + \lambda' f(x, u), \tag{7}$$

where λ is called the costate, $\lambda \in \mathbb{R}^n$, (x, λ) ranging in $2n$-dimensional phase-space. If $\mathscr{H}$ is assumed regular, then there exists a unique H-optimal control u^0, namely

$$u^0(x, \lambda) \triangleq \arg\min_u \mathscr{H}(x, \lambda, u), \tag{8}$$

and the derivative of $\mathscr{H}$ with respect to u vanishes at $(x,\ \lambda,\ u^0(x, \lambda))$.

Explicitly regular Hamiltonian means that the function $u^0(x, \lambda)$ is known (not only its existence but also its explicit form) and that it is sufficiently smooth on its variables. The control-Hamiltonian,

$$\mathscr{H}^0(x, \lambda) \triangleq \mathscr{H}(x, \lambda, u^0(x, \lambda)), \tag{9}$$

gives rise to the HCEs (see [21] for general problems; [22, p. 406], for the free final state case)

$$\dot{x} = \left(\frac{\partial \mathscr{H}^0}{\partial \lambda}\right)' \triangleq \mathscr{F}(x, \lambda), \quad x(0) = x_0, \tag{10}$$

$$\dot{\lambda} = -\left(\frac{\partial \mathscr{H}^0}{\partial x}\right)' \triangleq -\mathscr{G}(x, \lambda), \quad \lambda(T) = 2Sx(T), \tag{11}$$

which is a $2n$-dimensional ODE with a (Hamiltonian) vector field $\mathscr{X}$, explicitly

$$\begin{pmatrix} \dot{x} \\ \dot{\lambda} \end{pmatrix} \triangleq \dot{v} = \begin{pmatrix} \mathscr{F}(x, \lambda) \\ -\mathscr{G}(x, \lambda) \end{pmatrix} \triangleq \mathscr{X}(x, \lambda) = \mathscr{X}(v). \tag{12}$$

DOI: 10.1002/oca

Solutions to Equations (10, 11) result, under the hypotheses made, the optimal state and costate trajectories (denoted by $x^*(t)$ and $\lambda^*(t)$, respectively), which are also related through the value-function by (see [22])

$$\lambda^*(t) = \left(\frac{\partial \mathscr{V}}{\partial x}(t, x^*(t))\right)'. \tag{13}$$

The optimal control of Equation (8) is then explicitly constructed through

$$u^*(t) = u^0(x^*(t), \lambda^*(t)). \tag{14}$$

It is also useful to remind that the control-Hamiltonian is constant along the optimal trajectories, since

$$\frac{\mathrm{d}}{\mathrm{d}t}\mathscr{H}^0(x^*(t), \lambda^*(t)) = \left(\frac{\partial \mathscr{H}^0}{\partial x}\right)' \cdot \mathscr{F} + \left(\frac{\partial \mathscr{H}^0}{\partial \lambda}\right)' \cdot [-\mathscr{G}] = 0. \tag{15}$$

This property may be used to stabilize numerical calculations performed online (Equations (10, 11)), as is illustrated in [14], and when the optimal control law has no explicit form despite the problem being regular [23].

3.2. *The first-order quasilinear PDEs for missing boundary conditions*

Hamiltonian equations (10–11) pose a mixed-boundary-conditions problem, which has received much attention in applied mathematics and numerical analysis, leading to a variety of methods developed to approximate their solution. Invariant imbedding, one of the findings of Richard Bellman, attempts to include the missing final value of the state as a new variable and the time interval under consideration as a new parameter, into the flow of the original ODE (transition function for control systems), and take advantage of the smooth dependence of the flow on these variables and parameters whenever possible. Since the flow associated with a Cauchy problem with a C^n vector field is roughly $C^n (n \geqslant 1)$ in state variables, initial conditions, and parameters (see for instance [22, 24, 25]), then Bellman and Kalaba [26] extrapolated this result to the boundary-conditions situation and worked with the partial derivatives of the flow to obtain dynamic equations involving the boundary values and the optimization parameters. Here the missing initial values of the costates are added into the variables, and the final penalty coefficient into the parameters. In the Appendix (as an illustration), the arising PDEs relating the augmented set of variables and parameters for a linear system and quadratic criterion are presented (see [27] for more details). For a proof in the nonlinear general case, [16, 17] can be consulted. Some numerical aspects and applications of the 1-dimensional nonlinear case have been worked out in [14, 23].

Let us call $\rho(T, S) \triangleq x^*(T)$ the optimal final value of the state x, and $\sigma(T, S) \triangleq \lambda^*(0)$ the optimal initial value of the costate λ, both corresponding to a given (T, S)-optimal control problem. Let us also define

$$F(\rho, S) \triangleq \mathscr{F}(\rho, 2S(\rho - \bar{x})), \quad G(\rho, S) \triangleq \mathscr{G}(\rho, 2S(\rho - \bar{x})), \tag{16}$$

and

$$\begin{pmatrix} \alpha(T, S) \\ \beta(T, S) \end{pmatrix} \triangleq U(T, S) \begin{pmatrix} I \\ 2S \end{pmatrix} \tag{17}$$

where U is the inverse of the derivative of the flow associated with the Hamiltonian vector field ([17], see also Equations (A3–A4) in the Appendix). Exploiting the properties of the flow associated with the HCEs, then the following matrix equations arise for auxiliary $n \times n$ matrices α, β:

$$\begin{pmatrix} \alpha_T \\ \beta_T \end{pmatrix} = \begin{pmatrix} \alpha_S \mathscr{M}(\rho, S) - \alpha \mathscr{N}(\rho, S) \\ \beta_S \mathscr{M}(\rho, S) - \beta \mathscr{N}(\rho, S) \end{pmatrix}, \tag{18}$$

DOI: 10.1002/oca

where (α_T, β_T) and (α_S, β_S) are the partial derivatives of (α, β) with respect to the time horizon (T) and the final penalization coefficient (S), respectively. This notation will be used to define the partial derivatives of functions in order to simplify the equations. The matrices $\mathscr{M}(\rho, S), \mathscr{N}(\rho, S)$ take the form

$$\mathscr{M} \triangleq \tfrac{1}{2}(2\mathscr{A}'_1 S - \mathscr{A}'_3) + S(2\mathscr{A}'_2 S - \mathscr{A}'_4), \tag{19}$$

$$\mathscr{N} \triangleq 2\mathscr{A}'_2 S - \mathscr{A}'_4 \Rightarrow \mathscr{M} = \tfrac{1}{2}(2\mathscr{A}'_1 S - \mathscr{A}'_3) + S\mathscr{N}. \tag{20}$$

The submatrices $\mathscr{A}'_i$ are calculated from Equation (12) as

$$\mathscr{A}(T, S) \triangleq D\mathscr{X}(\rho, 2S(\rho - \bar{x})) = \begin{pmatrix} \mathscr{A}_1(\rho(T, S), S) & \mathscr{A}_2(\rho(T, S), S) \\ \mathscr{A}_3(\rho(T, S), S) & \mathscr{A}_4(\rho(T, S), S) \end{pmatrix}, \tag{21}$$

where $D\mathscr{X} = \partial\mathscr{X}/\partial v$, i.e. the derivative of the vector field $\mathscr{X}$, for details see [17]. The main matrix PDEs in Equation (18) are subject to the initial conditions

$$\alpha(0, S) = I, \quad \beta(0, S) = 2S. \tag{22}$$

Another set of PDEs for (ρ, σ) can be obtained [17]:

$$\begin{pmatrix} \sigma_T \\ 0 \end{pmatrix} = \begin{pmatrix} \beta_S\left(SF + \dfrac{G}{2} + \rho\right) - \beta(F - \rho_T - \rho_S) - \sigma_S \\ \alpha_S\left(SF + \dfrac{G}{2} + \rho\right) - \alpha(F - \rho_T - \rho_S) \end{pmatrix}, \tag{23}$$

and these become solvable when coupled to the matrix PDEs in Equation (18) for α, β, and subject to initial conditions

$$\rho(0, S) = x_0, \tag{24}$$

$$\sigma(0, S) = 2S(x_0 - \bar{x}). \tag{25}$$

On the existence and uniqueness of solutions to the coupled system of Equations (18, 23), there exist local results (see [25, p. 51]). The field of vector and matrix PDEs integration is in active development (see for instance [28]). A Picard type of algorithm is under development. Solutions ρ, σ will cover a whole range of parameter values. The usefulness of imbedding an individual problem into a (T, S)-family becomes evident from these solutions, because:

(i) the value ρ of the final state is revealed for each (T, S)-problem without the need to compute its optimal state trajectory, indicating how near to the desired value $\bar{x}$ the system will really end up under each set of parameter values. This allows to assess or modify the values of both T and S at the modeling/design level.
(ii) the initial value σ of the costate is a measure of the marginal cost $(\partial\mathscr{V}/\partial x)(0, x_0)$, where $\mathscr{V}$ is the value function (or Bellman function) of the problem, defined in Equation (4). Therefore, knowing $\sigma(T, S)$ will allow to estimate the effect on the total cost of the perturbations/uncertainties of the initial state for each parameter set, and hence helping in the choice of appropriate (T, S) values.

4. CSTR OPTIMAL TRAJECTORY GENERATION

This section describes a change of set-point from a stable equilibrium to another, corresponding to different flow rate values. The initial state

$$x_0 = \begin{pmatrix} 0.8283 \\ 1.0 \end{pmatrix} \tag{26}$$

DOI: 10.1002/oca

has an equilibrium flow rate $q_0 = 1.68812$, which exhibits input–output multiplicity, see Figure 3. The target is $\bar{x} = x_a = (0.9316 \;\; 0.5014)'$ corresponding to $\bar{u}_a = 0$ (or $q_0 = 3$ according to Figure 3). All control values will be taken relative to this $q_0 = 3$. The cost function $\mathscr{J}$ adopted here is the typical quadratic optimality criterion with finite time horizon T and final penalization matrix S, namely

$$\mathscr{J}(u) = \int_0^{\mathrm{T}} [(x(t)-\bar{x})' Q(x(t)-\bar{x}) + Ru^2(t)]\,\mathrm{d}t + (x(T)-\bar{x})' S(x(T)-\bar{x}), \tag{27}$$

which embodies a compromise between 'go as close as possible to the desired steady-state $\bar{x}$' and 'use a control as close as possible to the corresponding equilibrium value $\bar{u}$'. In this formulation, $Q \geqslant 0 \in \mathbb{R}^{2\times 2}$ penalizes state errors, $R > 0 \in \mathbb{R}$ penalizes the input effort and $S \geqslant 0 \in \mathbb{R}$ penalizes terminal state deviations from the target. For calculations $Q = 30 I_{2\times 2}$, $R = 4$, and $\bar{x} = x_a$. The Hamiltonian $\mathscr{H}$ results

$$\begin{aligned}\mathscr{H}(x,\lambda,u) = {} & 30(x_1-\bar{x}_1)^2 + 30(x_2-\bar{x}_2)^2 + 4u^2 + \cdots \\ & + \lambda_1\left(-\theta x_1 \exp\left(\frac{x_2}{1+x_2/\gamma}\right) + (q_0+u)(x_{1f}-x_1)\right) + \cdots \\ & + \lambda_2\left(\theta\beta x_1 \exp\left(\frac{x_2}{1+x_2/\gamma}\right) - \delta x_2 - (q_0+u)x_2\right).\end{aligned} \tag{28}$$

The optimal control (Equation (8)), extracted from the condition $(\partial\mathscr{H}/\partial u)(x,\lambda,u) = 0$, reads as

$$u^*(t) = \tfrac{1}{8}(\lambda_1^*(x_1^*-1) + \lambda_2^* x_2^*). \tag{29}$$

Equation (29) allows to calculate the optimal Hamiltonian $\mathscr{H}^0(x^*,\lambda^*)$, and to pose the Hamiltonian mixed-boundary-conditions problem equations (10–11), and to construct the corresponding PDEs developed in Section 3.2.

In Figures 4 and 5, common solutions of PDEs (23) are shown for a time horizon $T = 2$ and final penalization S ranging in $[0, 10]$. These figures illustrate how both, the final state and initial costate, change for different pairs (T, S). It must be clarified that these changes are not temporal evolutions from the differential equations (12) (see [16] for instance).

For most cases, to take large S-values will reduce the final error between the desired and the final states coming from PDE's solution, but this involve a greater total costs $\mathscr{J}$ in general. Additional

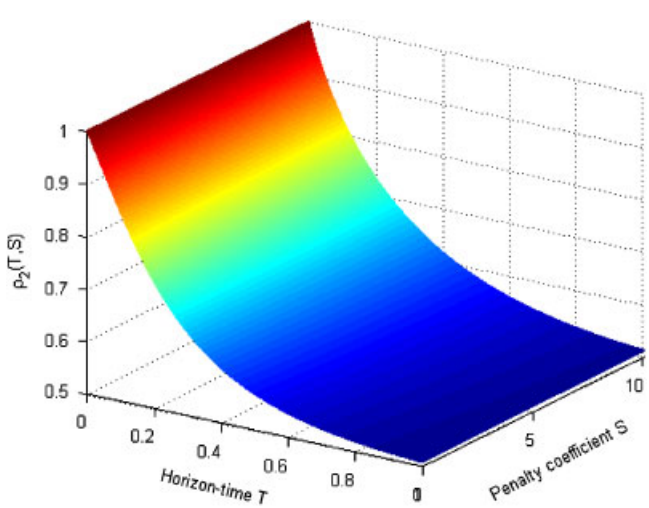

Figure 4. $\rho_2(T, S)$ final observed state for the change of set-point problem.

DOI: 10.1002/oca

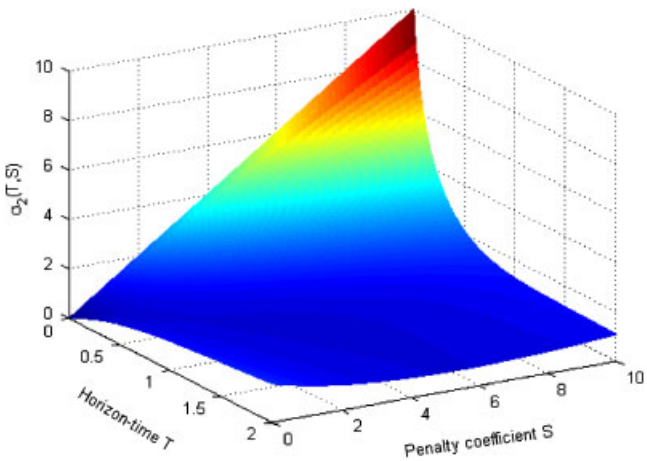

Figure 5. $\sigma_2(T, S)$ initial costate for the change of set-point problem.

information can be extracted from the PDE's solutions. For instance, a corrective control for small deviations of the optimal trajectory will be constructed based on the auxiliary matrices α, β coming from the definition (17) (see Equation (A18) below and [17] for more details).

The pair $(T, S) = (1.0, 3.5)$ was chosen for numerical evaluations concerning the change-of-set-point problem. The final states recovered from the PDE's solution corresponding to $T = 1.0$ and $s = 3.5$ were $x_1 = 0.9275$, $x_2 = 0.504$ that satisfactorily agree with the desired states x_a. The initial costates calculated numerically were $\lambda_1 = 2.05784$ and $\lambda_2 = 5.19785$. The PDEs were solved with standard software (Mathematica and Matlab, separately).

Figure 7 shows the optimal evolution of the x_2 state (x_2 is naturally adopted as the output of the system) resulting from the integration of HCEs with initial conditions. Clearly, x_2 arrives very near to its target.

Different control strategies (depicted in Figure 6) were applied to the system for comparison against the optimal control u^*. The resulting state trajectories have been plotted in Figure 7, and the cumulative and total costs corresponding to each case were plotted in Figure 8. The alternative controls tested were

$$u_1(\tau) = \begin{cases} 0.5 & \text{for } \tau \in [0, 0.7), \\ 0.0 & \text{for } \tau \in [0.7, 1), \end{cases} \qquad u_2(\tau) = 0 \ \forall \tau,$$

and $u_3(\tau)$ was a 'ladder type' function with intermediate values between the initial and final values of $u^*(\tau)$. The relative offset error for the optimal state trajectories was of the order of 0.3%, and higher for the others. The optimal control trajectory shows a classical behavior of finite-time optimization [29], i.e. it takes relatively high values at the beginning and the end of the optimization period. High initial values may be due to high penalization of state deviations in the trajectory cost expression (being coefficient $Q = 30I$), and after the deviation decreases, u^* decreases too because the control cost becomes important (being its coefficient $R = 4$). But the final penalization makes the control rise again, more than 0.15 above the expected final equilibrium value $\bar{u}_a = 0$. In the enlarged windows of Figure 8, the jump from trajectory cost to final cost at $\tau = 1$, i.e. the final penalization, is illustrated for the different strategies.

An attempt to treat the problem along the lines of 'Model Predictive Control' (MPC) was done through the 'Multi-Parametric toolbox' (MPT) for Matlab. The resulting control strategy is depicted in Figure 9, together with the evolution of the corresponding differential cost, compared with the optimal obtained from the paper's approach. As expected, the final MPC cost is bigger than the optimal one, although it grows at a slower pace during an initial period. The objective cost functional used in the comparison was the same (quadratic) for both techniques. The computational

DOI: 10.1002/oca

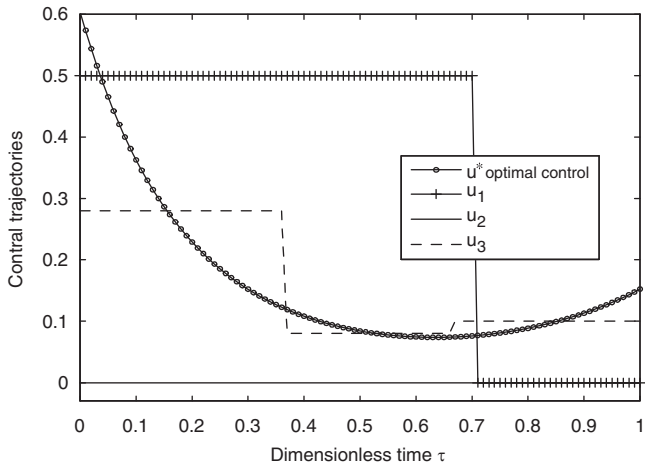

Figure 6. Some control trajectories used to compare against the optimal control.

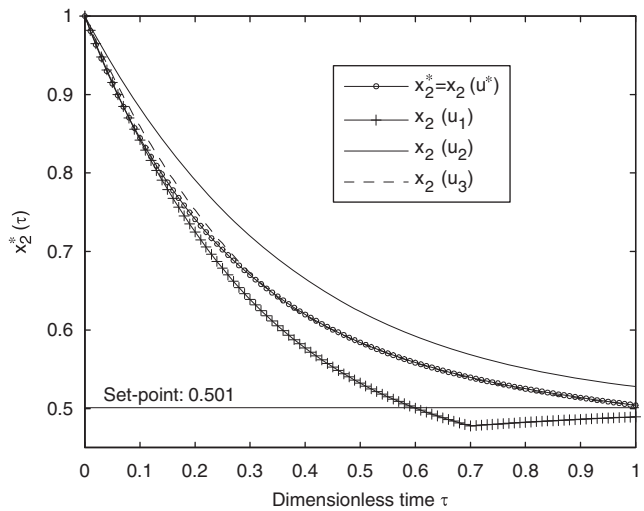

Figure 7. $x_2(\tau)$ state trajectories corresponding to control strategies in Figure 6.

efforts were compared as follows:

(i) For MPC, the reported calculation time for an average 'prediction horizon' equal to the 'control horizon' equal to 50 was 55 s. The online control effort cannot be adequately measured. The generation of the state trajectory was fast, but compensation actions and/or recalculations due to states' mismatching are not available with this package.

(ii) For the PDE's approach, the off-line calculation time was 9 s. The online complete trajectory (including compensation as in Figures 10 and 11) was generated in 15 s, well below the characteristic time $t_c = 60$ s, which shows that the method can be successfully implemented in-parallel with the given system.

5. ONLINE COMPENSATION OF PERTURBED OPTIMAL TRAJECTORIES

5.1. Hamiltonian linearization and feedback compensation

Optimal state solution $x^*(\cdot)$ coming from HCEs' integration provides a desired or reference state-trajectory generated by the open-loop optimal control $u^*(\cdot)$. But at any t time, the state $x(t)$ of

DOI: 10.1002/oca

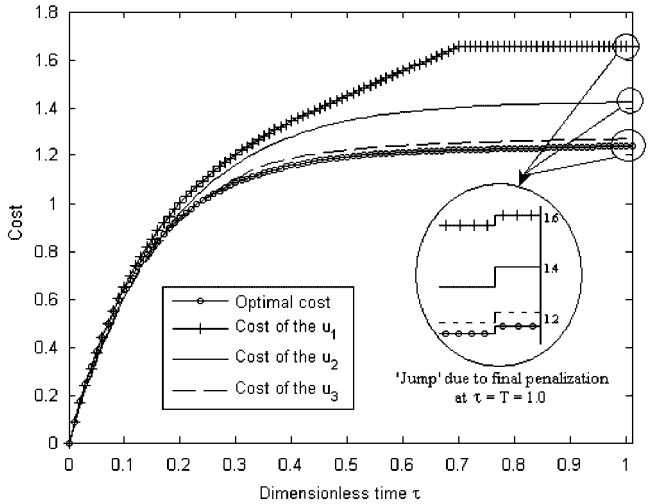

Figure 8. Cost trajectories and cumulative costs shown at $\tau = 1.0$ corresponding to control strategies in Figure 6.

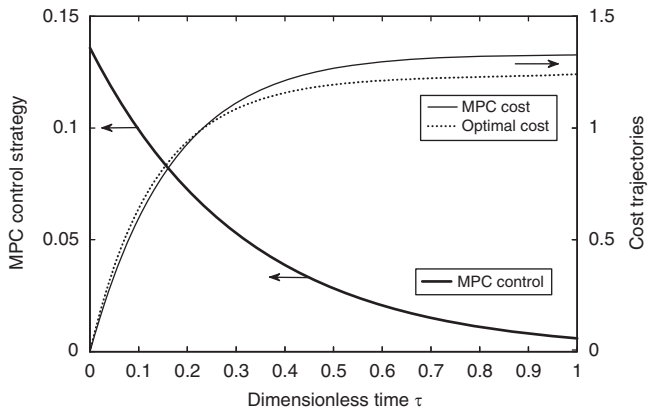

Figure 9. Comparison between the MPC and the optimal cost evolutions. The MPC control trajectory is also depicted, with values in the left axis.

the real system may differ from $x^*(t)$ due to perturbations in the signals. To annihilate the effect of these perturbations, a deviation control $\hat{u}(\cdot)$ may be added to the $\mathscr{H}$-optimal control $u^*(\cdot) = u^0$ calculated from Equation (29). If perturbations are relatively small, then the 'optimal' deviation variables

$$\hat{x}(t) \triangleq x(t) - x^*(t), \quad \hat{\lambda}(t) \triangleq \lambda(t) - \lambda^*(t), \quad t \in [0, T] \tag{30}$$

must approximately follow the dynamics, when the notation is simplified:

$$\begin{aligned} \dot{\hat{x}}(t) &= \dot{x}(t) - \dot{x}^*(t) = f(x, u^0(x, \lambda)) - f(x^*, u^0(x^*, \lambda^*)) \\ &\approx (f_x + f_u u_x^0)\hat{x}(t) + f_u u_\lambda^0 \hat{\lambda}(t), \end{aligned} \tag{31}$$

$$\begin{aligned} \dot{\hat{\lambda}}(t) &= \dot{\lambda}(t) - \dot{\lambda}^*(t) = -\left[\frac{\partial \mathscr{H}}{\partial x}(x, u^0(x, \lambda)) - \frac{\partial \mathscr{H}}{\partial x}(x^*, u^0(x^*, \lambda^*)\right]' \\ &\approx -[(\mathscr{H}_{xx} + \mathscr{H}_{xu} u_x^0)\hat{x}(t) + (f_x - u_\lambda^0 \mathscr{H}_{uu} u_x^0)' \hat{\lambda}(t)]', \end{aligned} \tag{32}$$

where $u_x^0 = -\mathscr{H}_{uu}^{-1} \mathscr{H}_{ux}$ and $u_\lambda^0 = -\mathscr{H}_{uu}^{-1} f_u'$ (calculated from the derivatives of the optimal condition $\mathscr{H}_u(x, \lambda, u^0(x, \lambda)) = 0$ with respect to x and λ, respectively), and where all partial derivatives of

DOI: 10.1002/oca

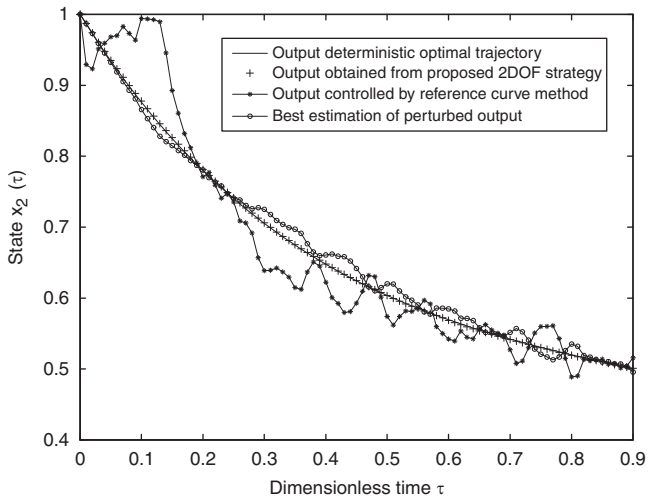

Figure 10. State x_2 trajectories.

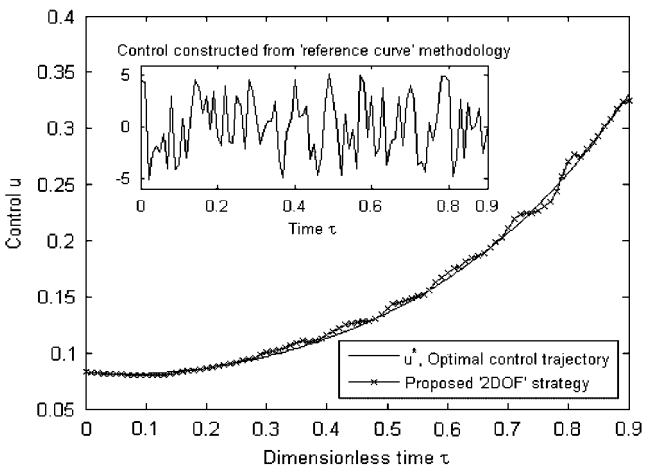

Figure 11. Control strategies for one-and two-degrees-of-freedom control.

$\mathscr{H}$, f, u^0 are evaluated along the nominal optimal trajectories $(x^*(t), \lambda^*(t))$. In this case-study, some of these expressions take the form:

$$f_x = \begin{bmatrix} -(q_0+u^*)-\theta E & -\theta x_1^* E\Gamma^2 \\ \theta\beta E & -(q_0+\delta+u^*)+\theta\beta x_1^* E\Gamma^2 \end{bmatrix}, \tag{33}$$

$$\Gamma \triangleq \frac{\gamma}{\gamma+x_2^*}, \quad E \triangleq \exp(x_2^*\Gamma), \quad u^* = u^0(x^*, \lambda^*), \tag{34}$$

$$f_u = \begin{bmatrix} 1-x_1^* \\ x_2^* \end{bmatrix}, \quad \mathscr{H}_{uu} = 8 = 2R, \quad \mathscr{H}_{ux} = [-\lambda_1^* \ \ -\lambda_2^*]. \tag{35}$$

And consequently the system expressed in (31–32) can be rewritten up to first-order system as (see Equation (21) and [17] for instance)

$$\begin{pmatrix} \dot{\hat{x}} \\ \dot{\hat{\lambda}} \end{pmatrix} = \tilde{\mathbf{H}} \begin{pmatrix} \hat{x} \\ \hat{\lambda} \end{pmatrix}, \tag{36}$$

DOI: 10.1002/oca

where

$$\tilde{\mathbf{H}} = \mathscr{A}(t,S) = DX = \frac{\partial \mathscr{X}}{\partial \hat{v}}(x^*(t),\lambda^*(t)) = \begin{pmatrix} \tilde{A} & -\frac{1}{2}\tilde{W} \\ -2\tilde{Q} & -\tilde{A}' \end{pmatrix}, \tag{37}$$

with

$$\tilde{A}(t) \triangleq f_x - f_u \mathscr{H}_{uu}^{-1} \mathscr{H}_{ux}, \tag{38}$$

$$\tilde{W}(t) \triangleq 2[f_u \mathscr{H}_{uu}^{-1} f_u'], \tag{39}$$

$$\tilde{Q}(t) \triangleq \tfrac{1}{2}[\mathscr{H}_{xx} - \mathscr{H}_{xu}\mathscr{H}_{uu}^{-1}\mathscr{H}_{ux}], \tag{40}$$

which is an ordinary linear time-variant differential equation. Following this line of reasoning, the optimal control deviation $\hat{u} \triangleq u - u^*$ may be approximated by

$$\hat{u} \approx u_x^0 \hat{x} + u_\lambda^0 \hat{\lambda} \approx -\mathscr{H}_{uu}^{-1}(\mathscr{H}_{ux}\hat{x} + f_u'\hat{\lambda}). \tag{41}$$

It is known that, for system (36) with

$$\hat{x}(0) = \hat{x}_0$$

$$\hat{\lambda}(T) = 2\tilde{S}\hat{x}(T)$$

boundary conditions, the costate deviation is

$$\hat{\lambda} = 2\tilde{P}(t)\hat{x}, \tag{42}$$

with $\tilde{P}(t)$ solution of the Riccati differential equation (DRE)

$$\dot{\tilde{P}}(t) = -(\tilde{P}\tilde{A} + \tilde{A}'\tilde{P} + \tilde{Q} - \tilde{P}\tilde{W}\tilde{P}), \quad \tilde{P}(T) = \tilde{S} = S, \tag{43}$$

and the control law for the deviations of optimal trajectory can be expressed in feedback form

$$\hat{u} = -\mathscr{H}_{uu}^{-1}(\mathscr{H}_{ux} + 2f_u'\tilde{P}(t))\hat{x}. \tag{44}$$

As a result, the total control reads

$$u(t) = u^*(t) + \hat{u}(t) = u^0(x^*(t),\lambda^*(t)) - \mathscr{H}_{uu}^{-1}(\mathscr{H}_{ux} + 2f_u'\tilde{P}(t))\hat{x}. \tag{45}$$

The final condition in Equation (43) seems to preclude the control strategy to be evaluated online, but considering the meaning of the auxiliary matrices (α, β) in Section 3.2 and their relationship with the matrix $U(T,S)$, which is the inverse to the fundamental solution of the system (36), then the initial condition $\tilde{P}(0)$ can be calculated as (see the Appendix)

$$\tilde{P}(0) = \tfrac{1}{2}\beta(T,S)\alpha^{-1}(T,S). \tag{46}$$

Therefore, for each (T,S) problem, the initial condition (46) allows to integrate the DRE online together with the calculation of all objects in the strategy.

5.1.1. Noise in I/O signals. Suboptimal compensation. Disturbances will be reinterpreted as signal noises in this subsection. In other words, the linear system given by (31) will model the deviation system, but since $x(t)$ is now a stochastic process, an estimation of $\hat{x}$ will be needed. In short, the dynamics of the deviation $\hat{x}$ from output measurements y will be

$$\dot{\hat{x}} = \tilde{A}(t)\hat{x}(t) - \tfrac{1}{2}\tilde{W}(t)\hat{\lambda}(t) + r_1, \tag{47}$$

$$\hat{y} = C\hat{x} + r_2 = y - Cx^*, \tag{48}$$

where, as usual, r_1 and r_2 are stochastic differentials of Brownian motions (i.e. the r_i may be considered as zero-mean Gaussian white noises) with covariance matrices σ_1 and σ_2, respectively. For the CSTR example proposed in Section 2, $C = (0\ 1)$.

DOI: 10.1002/oca

According to Equations (36–40, 42), the stochastic deviation process will be rewritten as

$$\dot{\hat{x}} = \hat{A}(t)\hat{x}(t) + r_1, \tag{49}$$

with

$$\hat{A}(t) \triangleq \tilde{A}(t) - \tilde{W}(t)\tilde{P}(t). \tag{50}$$

In this context, a Kalman–Bucy filter for the approximated model is optimal, and can be implemented through [19, 22, 30]

$$\dot{\hat{x}}(t) = \hat{A}(t)\hat{x}(t) + G(t)[\hat{y} - C\hat{x}], \quad \hat{x}(0) = \mathbb{E}(x_0) = x_0, \tag{51}$$

where the notation $\hat{x}$ is also used for the estimation of the stochastic deviation for simplicity, and where $G(t) \triangleq \Pi(t)C'\sigma_2^{-1}$, and $\Pi(t)$ is the solution to another Riccati-type ODE, integrable as an initial-value problem

$$\dot{\Pi}(t) = \hat{A}(t)\Pi + \Pi\hat{A}(t)' - \Pi C' C_2^{-1} C\Pi + C_1, \quad \Pi(0) = \mathrm{Cov}(x_0), \tag{52}$$

where $C_1 \triangleq \sigma_1\sigma_1'$, $C_2 \triangleq \sigma_2^2$.

Now, the optimal control strategy is complete (see the flow-sheet for 2DOF strategy in Figure 12 below). It was applied to an CSTR change of set-point problem similar to the one proposed in Section 4, and the results are shown in Figures 10, 11. Also, for comparison purposes, another control strategy called 'the curve reference method' in the literature (see [31] and the references therein) was implemented to cope with perturbations. The implicit purpose of the curve reference method is to isolate the dynamics of the manipulated variable from the main time-variable behavior that characterizes the operation, by taking the time evolution of a previous run as a reference. This attempts to cancel out most of the nonlinearities, capturing the dominant manipulated-variable dynamics by using empirical tuning rules for integrating systems [32]. Following the recipe in [31], a proportional positive gain was calculated ($k_c = 10.38$) and introduced in the reference curve feedback control law $\hat{u}_c$ for the tracking component

$$\hat{u}_c = -k_c(y(t) - y^*(t)) = -k_c\hat{y}(t). \tag{53}$$

Figure 10 shows several x_2 trajectories due to the application of the whole strategy proposed so far (considering noises and perturbations) to a change of set-point problem with the following parameters: $\bar{u}_0 = 1.3119$, $\bar{u}_a = 0$, $Q = I$, $R = 4$, $S = 3I$, $\bar{x} = x_a$, and

$$x_0 = \begin{pmatrix} 0.8283 \\ 1.0 \end{pmatrix}.$$

The solid line is the deterministic trajectory to track. The filtered x_2 trajectory is depicted with '+' mark and turns to be almost indistinguishable from the optimal trajectory. The line marked with '$\circ$' describes the best estimation of perturbed state $\hat{x} = x - x^*$ and the comparative trajectory x_2 controlled by the reference curve method is shown with the marked '$*$'.

Figure 11 shows the total control trajectories. The performance of the comparative scheme is not good. The control action $\hat{u}_c$ is oscillating in the range $-5 \leqslant u \leqslant 5$, which in a real application could create saturation levels for the actuator. Moreover, in many cases $\hat{u}_c$ produces unfeasible controls u (since u cannot take smaller values than -3 because it physically represents a deviation from a fixed flow rate $q_0 = 3$, for the change of set-point problem considered), but this was expected due to the fact that the method was not conceived for dealing with this sort of perturbations. This clearly shows the need to add the filtered stage.

5.1.2. '2DOF' flow-sheet. The flow-sheet shows the entire strategy devised in this paper and condensed in a 2DOF form. In a nonlinear setting, 2DOF control design uncouples the trajectory generation and asymptotic tracking problems. The first problem was solved through the HCEs. The resulting reference trajectory $x^*(t)$ is the optimal state solution over a finite horizon T and

DOI: 10.1002/oca

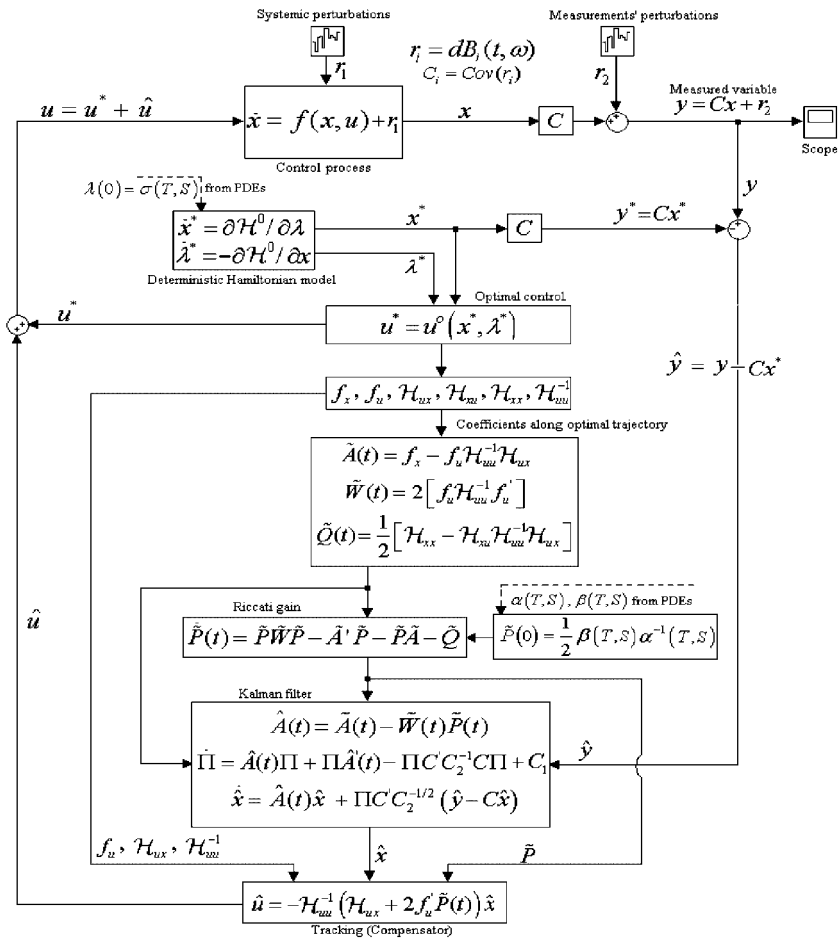

Figure 12. Flow-sheet for 2DOF strategy.

corresponding to a final matrix penalization S (see Section 3, [16], and their references). The deviation system (represented by Equation (36)) is then written as a linear time-varying control system (Section 5.1) in terms of its output $\tilde{y} = y - Cx^*$. However, this output deviation is corrupted by systemic and measurement perturbations, and needs additional control (the second degree of freedom). This is equivalent to attempt to track the reference optimal trajectory. The asymptotic tracking problem requires two blocks: the Kalman–Bucy filter, which is responsible for providing the best estimation of $x - x^*$ (Section 5.1.1), and the generation of the Riccati gain $\tilde{P}(t)$. With $\tilde{P}$ and $\hat{x}$, the optimal stochastic feedback law results Equation (44).

6. CONCLUSIONS

A 2DOF methodology has been developed for the control of nonlinear processes and is illustrated through the treatment of classical problems arising in CSTRs. The main steps in applying the scheme are as follows:

(i) Off-line calculation of missing boundary conditions and auxiliary matrices for a (T, S) family of optimal control problems posed for the nonlinear dynamics. This amounts to solve a set of first-order quasilinear PDEs (Equations 18–23), which actually may be reduced to solve an initial-value problem for a related set of ODEs. These initial calculations can

DOI: 10.1002/oca

be considered as the 'controller design' stage, and the results are stored to treat individual situations once the values of T and S are chosen from inspection of $\rho(T, S)$.

(ii) The nominal optimal trajectory is generated by online integration of Hamiltonian equations of the optimal control problem (10, 11). This can be done thanks to the initial value of the costate λ, i.e. $\lambda(0)=\sigma(T, S)$, provided by the (i)-stage results. The integration of the Hamiltonian ODEs is equivalent to running a dynamic model of the system, and the resulting values $(x^*(t), \lambda^*(t))$ are necessary to generate the 'first-degree-of-freedom' component of the control strategy, i.e. $u^*(t)=u^0(x^*(t), \lambda^*(t))$. The optimal state $x^*(t)$ is then taken as an approximation to the real values $x(t)$ of the physical state variables, which in general are unknown or difficult to measure. The differences $\hat{x}(t)\cong x(t)-x^*(t)$ are assumed to be produced by systemic noise, i.e. by random interaction between the plant and the environment.

(iii) Since only output values $y(t)$ are available, usually corrupted by measurement noise, an estimation of the perturbation $\hat{x}(t)$ is constructed through a Kalman–Bucy filter (Equations 51–52). The setup is justified by the concept of 'perturbation', i.e. the differences $\hat{x}(t)$ are assumed to obey a linear time varying dynamics (Equation 36) with coefficients generated online (the nominal optimal trajectory acts as a 'reference curve' to be tracked).

(iv) The perturbation $\hat{x}(t)$ is abated by the action of 'second degree-of-freedom' component $\hat{u}(t)=-k(t)\hat{x}(t)$ or compensator (44). The gain includes a generalized Riccati matrix $\tilde{P}(t)$ (Equation 46), which is obtained from the (i)-stage results. This is possible because $\tilde{P}(0)$ depends only on matrices α, β, which by definition take care of the derivative of the Hamiltonian flow, i.e. of the linearization of the system along optimal trajectories $(x^*(t), \lambda^*(t))$. Notice that the availability of $\hat{P}(0)$ avoids the usual off-line integration of DRE that would have to be performed for each linear time-varying system with a finite optimization horizon T and a final penalty coefficient S. It should be remarked that the time-variant gain of the compensator (in Equation (44)) includes a term $\mathscr{H}_{uu}^{-1}\mathscr{H}_{ux}$ not visible in the usual LQR approach (compare with Equation (A21)). This is due to the fact that the unifying Hamiltonian approach is always referring to the original optimal control problem, which is nonlinear and with a non-necessarily quadratic Lagrangian. For a linear quadratic case, $\mathscr{H}_{ux}=0$. $f_u=B$, $\mathscr{H}_{uu}=2R$.

(v) The 2DOF control is then $u(t)=u^*(t)+\hat{u}(t)$. The application of this strategy results in a practically complete adherence to the nominal trajectory $x^*(t)$. A comparison against classical application of the 'reference curve' plus PI control is worked out for illustration.

As a whole, the scheme shows a very satisfactory behavior and combines the features of optimal approaches to both the deterministic nonlinear control of the model and the stochastic linear control of the perturbations.

APPENDIX A: PDES FOR MISSING BOUNDARY CONDITIONS AND CONTROL GAINS IN THE TIME-CONSTANT LQR CONTEXT

The Hamiltonian form of the LQR problem (with linear dynamics $f=Ax+Bu$ and quadratic Lagrangian $L=x'Qx+u'Ru$) reads

$$\dot{v}=\begin{pmatrix}\dot{x}\\ \dot{\lambda}\end{pmatrix}=\begin{pmatrix}A & -\frac{1}{2}W\\ -2Q & -A'\end{pmatrix}\begin{pmatrix}x\\ \lambda\end{pmatrix}=\mathbf{H}v, \tag{A1}$$

where

$$W\triangleq BR^{-1}B' \quad \text{and} \quad \mathbf{H}=\begin{pmatrix}A & -\frac{1}{2}W\\ -2Q & -A'\end{pmatrix}.$$

Therefore, in this case the HCEs become a linear, time-constant dynamical system with a vector field $\mathscr{X}(v)=\mathbf{H}v$, whose flow verifies

$$\phi^{\mathrm{T}}(v)=\mathrm{e}^{\mathbf{H}\mathrm{T}}v, \tag{A2}$$

DOI: 10.1002/oca

and consequently

$$V = D\phi^{\mathrm{T}} = \phi^{\mathrm{T}} = \mathrm{e}^{\mathbf{H}\mathrm{T}}, \tag{A3}$$

$$U = V^{-1} = \mathrm{e}^{-\mathbf{H}\mathrm{T}}. \tag{A4}$$

The Hamiltonian system being linear implies that solutions depend smoothly on parameters and initial conditions, and then derivatives of Equation (17) with respect to (T, S) can be taken as

$$\begin{pmatrix} \alpha_T \\ \beta_T \end{pmatrix} = -\mathbf{H}U \begin{pmatrix} I \\ 2S \end{pmatrix}, \tag{A5}$$

$$\begin{pmatrix} \alpha_S \\ \beta_S \end{pmatrix} = U \begin{pmatrix} 0 \\ 2I \end{pmatrix}. \tag{A6}$$

Now, by partitioning in the obvious way

$$U = \begin{pmatrix} U_1 & U_2 \\ U_3 & U_4 \end{pmatrix} \tag{A7}$$

allows Equation (A6) to read

$$\tfrac{1}{2}\alpha_S = U_2, \quad \tfrac{1}{2}\beta_S = U_4, \tag{A8}$$

which combined with Equation (17) gives

$$U_1 = \alpha - S\alpha_S, \quad U_3 = \beta - S\beta_S, \tag{A9}$$

and then, by inserting these results in Equation (A5), the following (main) relations are obtained:

$$\boxed{\alpha_T - \alpha_S \mathscr{M}(S) = -\alpha \mathscr{N}(S)}, \tag{A10}$$

$$\boxed{\beta_T - \beta_S \mathscr{M}(S) = -\beta \mathscr{N}(S)}, \tag{A11}$$

where $\mathscr{M}(S) \triangleq A'S + SA + Q - SWS$, $\mathscr{N}(S) \triangleq A - WS$.

Boundary conditions for a process of zero horizon are imposed, i.e.

$$\alpha(0, S) = I, \quad \beta(0, S) = 2S. \tag{A12}$$

Therefore, Equations (18) for α,β can be integrated alone, since they do not depend on ρ, σ. Actually, from

$$\begin{pmatrix} x_0 \\ \sigma \end{pmatrix} = \mathrm{e}^{-\mathbf{H}\mathrm{T}} \begin{pmatrix} \rho \\ 2S\rho \end{pmatrix} = U \begin{pmatrix} I \\ 2S \end{pmatrix} \rho = \begin{pmatrix} \alpha \\ \beta \end{pmatrix} \rho, \tag{A13}$$

it follows that no further equations are needed for ρ, σ. Since α is always invertible (see [22], p.371), then the missing boundary conditions result

$$\rho = \alpha^{-1} x_0, \tag{A14}$$

$$\sigma = \beta\rho. \tag{A15}$$

DOI: 10.1002/oca

Illustrations can be found in [27]. From Equation (13) for the LQR case, the initial costate has here the form

$$\sigma=\lambda^*(0)=\left(\frac{\partial\mathscr{V}}{\partial x}(0,x^*(0))\right)'=2P(0)x_0, \tag{A16}$$

where P is in turn the numerical solution of the DRE, i.e. of the final-value matrix ODE

$$\dot{\pi}=\pi W\pi-\pi A-A'\pi-Q, \quad \pi(T)=S. \tag{A17}$$

Therefore, from Equations (A14–A16), for each (T,S)-problem the Riccati matrix $P(t)$ should also verify

$$P(0)=\tfrac{1}{2}\beta(T,S)[\alpha(T,S)]^{-1}. \tag{A18}$$

The method based on PDEs for missing boundary conditions avoids solving the DRE (A17) for each particular (T,S)-problem, and storing, necessarily as an approximation, the Riccati matrix $P(t)$ for the values of $t\in[0,T]$ chosen by the numerical integrator, possibly different from the time instants for which the control $u(t)$ is constructed. Instead, the HCEs (A1) can be integrated with initial conditions

$$x(0)=x_0, \quad \lambda(0)=\sigma(T,S), \tag{A19}$$

and the optimal trajectories $x^*(t)$, $\lambda^*(t)$ obtained for $0\leqslant t\leqslant T$, which allows to generate the optimal control at each time

$$u^*(t)=u^0(x^*(t),\lambda^*(t))=-\tfrac{1}{2}R^{-1}B'\lambda^*(t), \tag{A20}$$

or, in this case, the feedback form, which becomes directly available due to the linear dependence of Equations (A14, A15) on initial conditions,

$$u^*(t)=-\tfrac{1}{2}R^{-1}B'\beta(T-t,S)[\alpha(T-t,S)]^{-1}x. \tag{A21}$$

REFERENCES

1. Strogatz SH. *Nonlinear Dynamics and Chaos*. Perseus Books Reading: MA, 1994.
2. Costanza V. A variational approach to the control of electrochemical hydrogen reactions. *Chemical Engineering Science* 2005; **60**:3703–3713.
3. Aris R. *Mathematical Modeling. A Chemical Engineer's Perspective* (specially Chapter 4: *Presenting the Model and its Behavior*). Academic Press: New York, 1999.
4. Sistu PB, Bequette BW. Model predictive control of processes with input multiplicities. *Chemical Engineering Science* 1995; **50**:921–936.
5. Bequette BW. Nonlinear control of chemical processes: a review. *Industrial Engineering Chemical Research* 1991; **30**:1391–1413.
6. Henson MA, Seborg DE. *Nonlinear Process Control*. Prentice-Hall: Englewood Cliffs, 1997.
7. Antonelli R. *Output Feedback Regulation of Nonlinear Chemical Processes with Input Constraints*. AIChE: New York, 1999.
8. Kumar A, Daoutidis P. *Control of Nonlinear Differential Algebraic Equations with Applications to Chemical Processes*. Chapman and Hall/CRC: London, 1999.
9. Qin SJ, Badgwell TA. A survey of industrial model predictive control technology. *Control Engineering Practice* 2003; **11**:733–764.
10. Camacho EF, Bordons C. *Model Predictive Control* (2nd edn). Springer: London, 2004.
11. Bequette BW. Non-linear model predictive control: a personal retrospective. *The Canadian Journal of Chemical Engineering* 2007; **85**:408–415.
12. Magni L, Raimonodo DM, Allgower F. *Nonlinear Model Predictive Control*. Springer: Berlin, Heidelberg, 2009.
13. Murray R. Optimization Based-control, California Institute of Technology, CA, 2009. Available from: http://www.cds.caltech.edu/~murray/amwiki/Supplement:_Optimization-Based_Control.
14. Costanza V, Rivadeneira PS. Finite-horizon dynamic optimization of nonlinear systems in real time. *Automatica* 2008; **44**:2427–2434.
15. Kravaris C, Wright R. Two-degree-of-freedom output feedback controllers for nonlinear processes. *Chemical Engineering Science* 2005; **60**:4323–4336.

DOI: 10.1002/oca

16. Costanza V. Finding initial costates in finite-horizon nonlinear-quadratic optimal control problems. *Optimal Control Applications and Methods* 2007; **29**:225–242.
17. Costanza V. Regular optimal control problems with quadratic final penalties. *Revista de la Unión Matemática Argentina* 2008; **49**:43–56.
18. Costanza V. Parametric uncertainty and disturbance attenuation in the suboptimal control of a nonlinear electrochemical process. *Optimal Control Applications and Methods* 2007; **28**:209–228.
19. Costanza V, Neuman CE. Optimal control of non-linear chemical reactors via an initial-value Hamiltonian problem. *Optimal Control Applications and Methods* 2005; **27**:2041–2053.
20. Uppal A, Ray WH, Poore AB. On the dynamic behavior of continuous stirred tank reactors. *Chemical Engineering Science* 1974; **29**:967–985.
21. Pontryagin LS *et al. The Mathematical Theory of Optimal Processes*. Wiley: New York, 1962.
22. Sontag ED. *Mathematical Control Theory* (2nd edn). Springer: New York, 1998.
23. Costanza V, Rivadeneira PS. Minimal-power control of electrochemical hydrogen reactions. *Optimal Control Applications and Methods* 2010; **31**:105–115.
24. Abraham R, Marsden JE. *Foundations of Mechanics* (2nd edn). Benjamin/Cummings: MA, 1978.
25. Folland GB. *Introduction to Partial Differential Equations* (2nd edn). Princeton University Press: Princeton, NJ, 1995.
26. Bellman R, Kalaba R. A note on Hamilton's equations and invariant imbedding. *Quarterly of Applied Mathematics* 1963; **XXI**:166–168.
27. Costanza V, Neuman CE. Partial differential equations for missing boundary conditions in the linear–quadratic optimal control problem. *Latin American Applied Research* 2009; **39**:207–212.
28. Zenchuk AI, Santini PM. Dressing method based on homogeneous Fredholm equation: quasilinear PDEs in multidimensions, 2007. Available from: http://arxiv.org/pdf/nlin/0701031.
29. Bryson A Jr, Ho Y. *Applied Optimal Control*, revised printing. Wiley: New York, 1975.
30. Fleming WH, Rishel RW. *Deterministic and Stochastic Optimal Control*. Springer: New York, 1975.
31. Marchetti JL. Referential process–reaction-curve for batch operations. *AIChE Journal* 2004; **50**:3160–3168.
32. Ziegler JG, Nichols NB. Optimum settings for automatic controllers. *Transactions of the ASME* 1942; **64**:759.

DOI: 10.1002/oca